Variational Analysis of Hydrometeors with Satellite Radiance Observations: A Simulated Study

Zhiquan Liu (liuz@ucar.edu), Xiaoyan Zhang, Thomas Auligné and Hui-Chuan Lin
National Center for Atmospheric Research, Boulder, CO, USA

Abstract

This study focuses on the assimilation of the simulated radiances using CRTM under cloud and precipitation conditions, both in an incremental 3DVAR and a non-incremental 1DVAR framework. In 3DVAR, a total water control variable and a warm-rain physics scheme are combined to allow the assimilation of cloud and precipitation affected radiances. Cloud and rain information can be to some extent extracted with this scheme by assimilating the simulated SSMIS radiances over a convective case. In 1DVAR, the control variables are the individual hydrometeors instead of the total water as in 3DVAR. No physical constraint is applied and a quasi-Newton algorithm is used for non-linear minimization. The 1DVAR retrieved hydrometeor profiles from the simulated radiances have a good fit with the "truth" when having a carefully specified observation and background error covariance.

1. Introduction

Assimilation of radiance measurements from a variety of satellite platforms is not new. NWP centers have been routinely or experimentally assimilating the clear-sky radiometric data as well as retrieved products (e.g., McNally et al., 2002). However, assimilating the radiances measured in cloudy and precipitating conditions is still very challenging even though improvements have recently been make in this area (e.g., Bauer et al., 2006). This study will investigate the efficiency and drawback of the variational techniques with the simulated radiances, which are affected by cloud and precipitation. The emphasized instrument is SSMIS, which combines some channels of AMSU-A, AMSU-B and SSMI and contains the channels sensitive to cloud liquid water and rain.

The paper is organized as follows. Next section will briefly describe a WRF model run for a convective case, which will serve as the "truth" for this simulated study. The simulated SSMIS radiances are obtained by using the model "truth" as the input of CRTM. The simulation results in a 3DVAR system are given in the section 3. In the section 4, the performance of hydrometeor profiles retrieval is evaluated in a 1DVAR framework with a variety of scenarios. The conclusions are summarized in the last section.

2. The model "truth" and the simulated SSMIS radiances

In the spring of 2008, NCAR/MMM had performed the near real-time convective forecasting initialized at 0000 UTC and 1200 UTC with a 9km/3km nested domain. Each forecast was initialized with a WRF-Var/WRF assimilation/forecast cycle starting from T-12h in a 9km resolution. We select the initial condition at 0000 UTC 8th May, 2008 as the "truth" for this simulated study. The Thompson microphysics scheme was used in the convective forecasts. Both liquid- and frozen-phase hydrometeors (cloud liquid water, rain, cloud ice, snow, graupel) were generated in the model "truth". However, only cloud water and rain are taken into account in the simulation, and the frozen hydrometeors are ignored due to the limitation of the current WRF-3DVAR (see the section 3). For speeding up the testing, the resolution is reduced to 27km and only a small domain (5550 grid points) covering the convective rain-band is cut out for the simulation. Figure 1 shows the column-integrated cloud water and rain in the model "truth". The SSMIS radiances (channels 1~6, 8~18) are simulated in each grid-point by applying CRTM to the model profiles (T, Q, cloud water and rain). Figure 2a gives the simulated channel 17 brightness temperatures, which are sensitive to the rain. A cold band is clearly consistent with the cloud/rain band. The domain averaged Tb difference between cloudy and cloud-free simulation for all channels is shown in Figure 2b, which indicates the channels' sensitivity to cloud and rain.

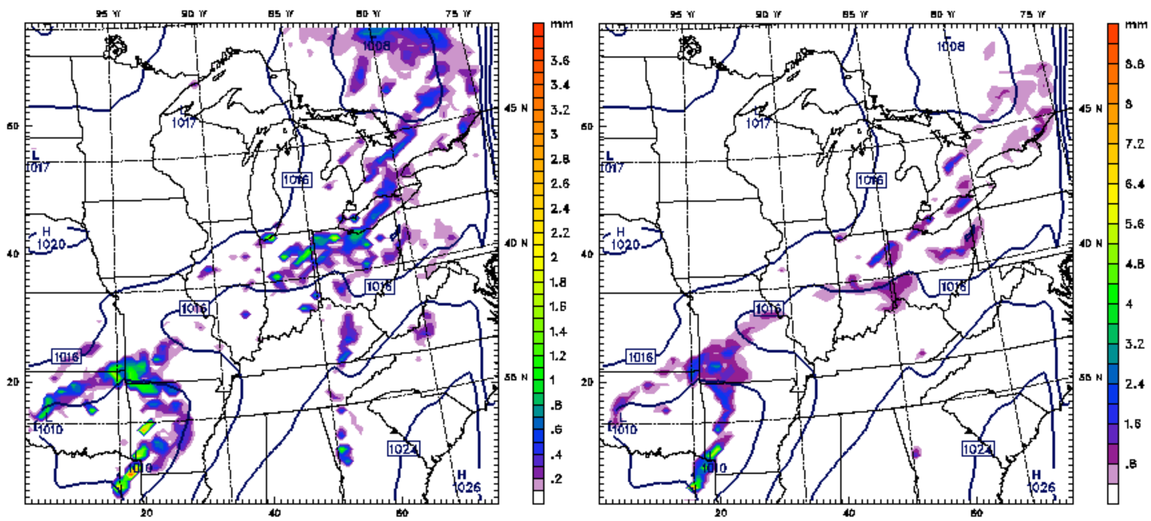

Figure 1. The column-integrated cloud water (left) and rain (right) in the model "truth".

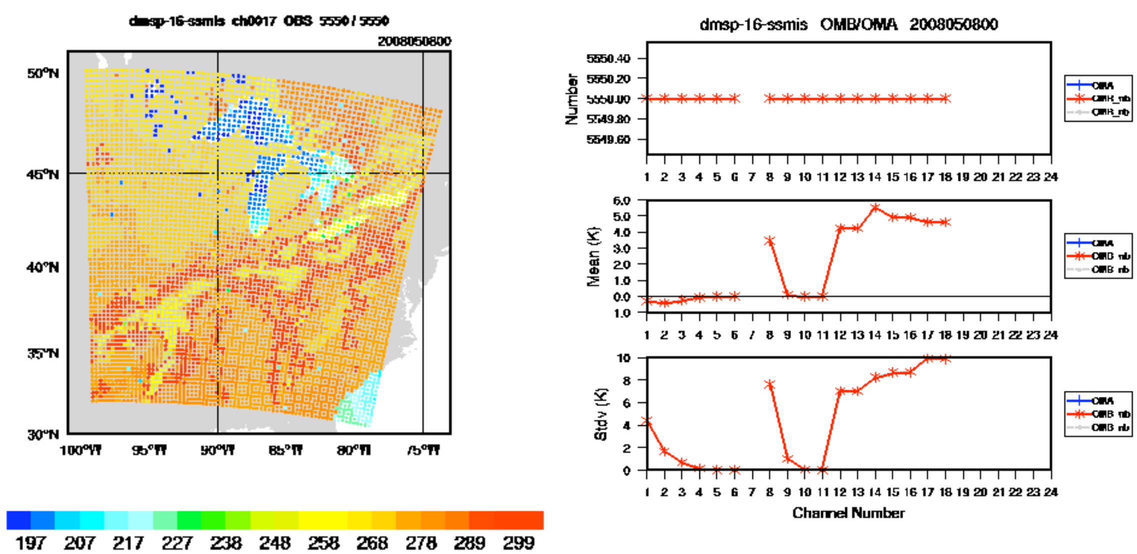

Figure 2. (a) The simulated SSMIS channel 17 brightness temperatures in each grid-point; (b) the domain averaged Tb difference between cloudy and cloud-free simulation for all SSMIS channels.

3. Simulation in a 3DVAR system

Radiance assimilation capability has been implemented in WRF-Var data assimilation system (Liu and Barker, 2006). Both CRTM and RTTOV were integrated into the WRF-Var for serving as the radiance observation operator. The users have flexibility to use CRTM or RTTOV through a simple namelist parameter. In the initial implementation, radiance data can be assimilated only in clear-sky (here "clear" is more in an optical sense) situations. Recently, this capability has been extended to assimilate radiances over cloudy and/or precipitating areas when using CRTM. The necessary changes for cloud/rain affected radiance assimilation include: (1) extending CRTM interface to include the hydrometeor profiles (cloud liquid water, cloud ice, rain, snow, graupel, hail) as the input; (2) replacing the usual moisture control variable with a total water control variable $Q_t=Q_{wv}+Q_{clw}+Q_{rain}$; (3) using TL and AD of a warm-rain physical scheme for partitioning Qt increment into individual Q_{wv}, Q_{clw} and Q_{rain} increment. A similar scheme (the Q_t control variable and the warm-rain constrain) has been also used for assimilating radar reflectivity (Xiao et al., 2007).

This cloudy radiance assimilation scheme was tested with the simulated SSMIS radiances for that convective case as described in the section 2. For the initial testing, the following scenario was considered for the simulation. The simulated observations are "perfect", i.e., no random noise was added in the observations. The background fields are considered to be cloud-free. This is an extreme scenario, yet still realistic in a real world. For instance, the cloud locations between the model forecast and observations are very likely mismatched. The background for other fields such as T and Q is also considered perfect, i.e., taking the "true" T, Q fields generating the simulated radiances as the background. This is an idealized situation, yet still reasonable to take in regard to our focus on the cloud/rain analysis and the dominant signal from cloud/rain contribution. For WRF-Var's iterations, we use two outer loops with the gradient reduction of 100 times as the convergence criterion in each loop. We simply adopt the Q background error covariance for Q_t but with a much smaller length scale (1/5 of Q's length scale) to take into account more localized cloud/rain fields.

Figure 3 shows the analyzed column-integrated cloud water (left panel) and rain (right panel) with assimilating the simulated SSMIS radiances. Comparing to the corresponding "truth" in Figure 1, both cloud water and rain are to some extent recovered from a cloud-free background. The analysis of rain is much better than that of cloud water both in terms of large pattern and the quantity of water content. Note that the same color scale was used in Figure 1 and 3. The analysis of the column-integrated rain is remarkably consistent with the "truth" except for some areas with extreme precipitation near the low-left corner of the domain. A major problem with the analysis of cloud water is that the cloud band was largely broadened comparing to the "truth". The reason for that is unclear. With a closer look at the vertical structure of cloud and rain, we found that the vertical consistency between the analysis and the "truth" is not as good as for the column-integrated quantity. Another issue is that T and Q increments are inevitable generated through the warm-rain constrain while creating cloud and rain increment. For some configurations (e.g., with a more strict convergence criterion and therefore more iterations), it can even produce very large unrealistic T and Q increments even though starting from a perfect T and Q background. This issue could be partly due to the inconsistency between the warm-rain physical constrain used in WRF-Var and the microphysics scheme (Thompson scheme) used for creating the simulation situation. Figure 4 gives also the cloud-free background and the analysis after the first outer loop in the brightness temperature space for SSMIS channel 17. It can be seen that the analyzed Tb has a clearly better fit to the simulated observations in Figure 2a.

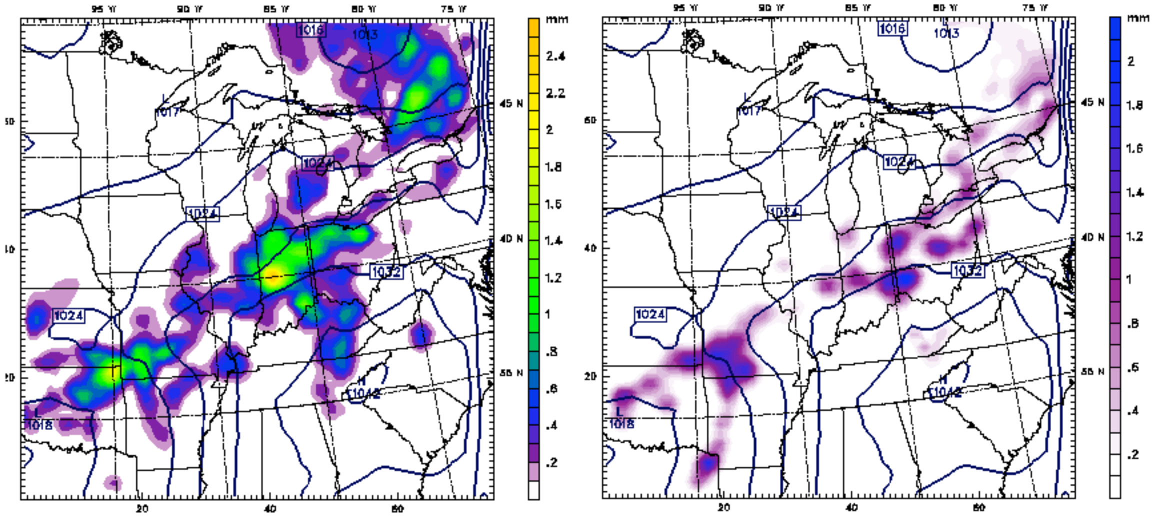

Figure 3. the analyzed column-integrated cloud water (left panel) and rain (right panel).

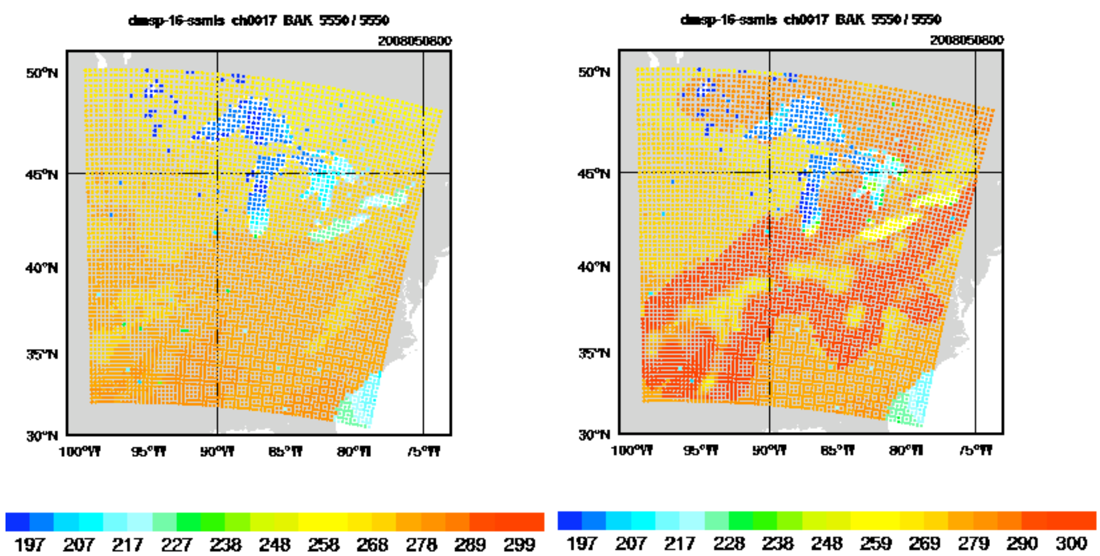

Figure 4. Left: Cloud-free background brightness temperatures for SSMIS channel 17; Right: the analyzed brightness temperatures for SSMIS channel 17 after the first outer loop.

It was noticed that the initial cost function and gradient are in the order of ~10^6 and ~10^5 due to the large innovation values for cloud/rain conditions. The configuration above (a gradient reduction of 10^{-2}) did not lead to a real convergence. Some other configurations (i.e., more outer loops, more strict convergence criterion) were tested for having a better convergence. However, these were less successful by creating unrealistic T, Q increments. Two factors might play the important role for the limitation of current cloudy radiance assimilation scheme in WRF-3DVAR: uncertainty of the warm-rain constrain and the incremental implementation of WRF-3DVAR. The latter are more appropriate for the problem with a relatively good background. It is worthwhile to explore the potential of adopting a non-incremental algorithm and using individual hydrometeors as the control variables without any physical constrain. This will be further investigated in a simplified 1DVAR framework in the next section.

4. Simulation in a 1DVAR framework

For better understanding the "physics" of cloudy radiance assimilation, a 1DVAR retrieval package has been developed with the emphasis on the retrieval under cloud/rain conditions. This 1DVAR package can serve as an independent research tool for the study of the advanced algorithms and of the radiance information content. It can be also extended to integrate into a 3DVAR/4DVAR system for some kinds of preprocessing or quality control steps. The components needed for 1DVAR are basically same as for 3DVAR, e.g., the observation (Tb) and background (T, Q, hydrometeor profiles) inputs as well as the corresponding error covariance matrices, CRTM as the observation operator and a minimization algorithm to find the minimum of the cost function. However, 1DVAR does not take into account the correlation between the pixels and multivariate correlation, and generally does not use other conventional observations. More specifically, this 1DVAR is a non-incremental implementation with a quasi-Newton minimization algorithm. It was designed to allow the individual hydrometeor profiles together with T and Q profiles as the control variables. No physical constraint is applied for the relationship among T, Q and hydrometeors. The observation errors are uncorrelated between channels and the background errors are vertically correlated for all T, Q and hydrometeor variables.

416 profiles with CLWP>0.2mm were selected from the same case as described in the sections 2 and 3. Those profiles correspond to the cloud/rain band as shown in Figure 1. The ensemble of 416 profiles for cloud water and rain are plotted in Figure 5. Similar to the simulation in the 3DVAR, those model profiles are considered as the "truth". Again, SSMIS radiances are simulated by ingesting those profiles into CRTM.

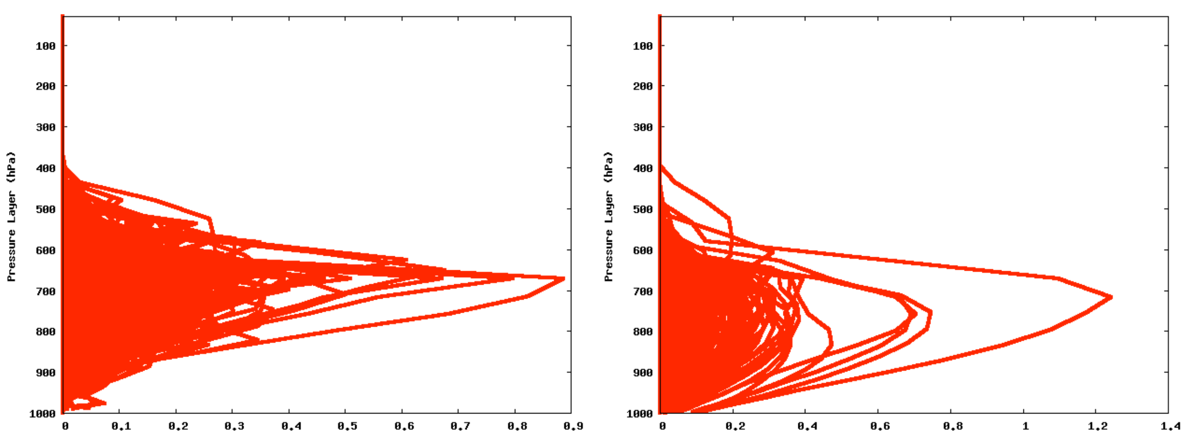

Figure 5. The ensemble of 416 profiles for cloud water (left) and rain (right), selected from the same case in the section 2.

The first scenario considered for 1DVAR cloud/rain retrieval is very similar to that in 3DVAR. The control variables are T, Q, cloud water and rain profiles. The simulated radiance observations are considered as "perfect", i.e., no random errors are added in the observations.

1DVAR iterations start from a cloud-free background but with the "perfect" T and Q background. The retrieval results of cloud and rain for all 416 profiles are shown in the Figure 6. The "true" profiles are shown in red curves and the corresponding retrievals in green curves. We can see that rain profiles are overall well retrieved except for some heavy rain conditions. However, the retrieval of cloud water is much more underestimated. This seems to be consistent with the results in the 3DVAR simulation, where the analysis of rain is also better than that of cloud water. It should be mentioned that at minimum a great reduction in the initial cost function ($\sim 10^4$) and the gradient ($\sim 10^5$) was observed ($10^{-2}/10^{-4}$) and the analyses in Tb space almost perfectly converge to the observations (not shown) even with very large innovation values. This indeed requires a great number of iterations to reach that convergence level. A more efficient minimization algorithm and/or a better preconditioning shall improve 1DVAR's convergence efficiency. Not like in the 3DVAR simulation with a physical constraint, no unrealistic large T and Q increments are observed with large number of iterations.

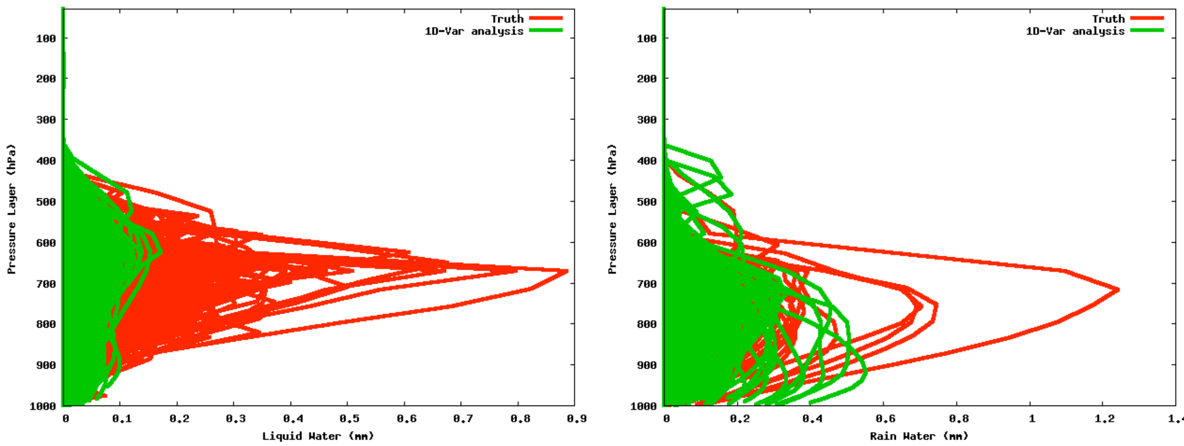

Figure 6. The retrieval results of cloud and rain for all 416 profiles. The "true" profiles are shown in red curves and the corresponding retrievals in green curves.

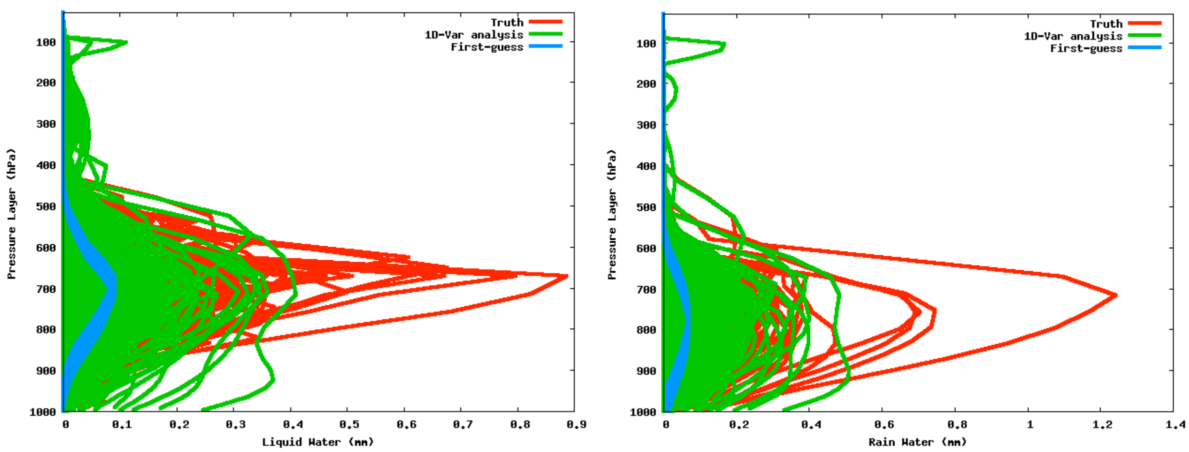

Figure 7. Same as in Figure 6, but with a different scenario. See text for more details.

In the second scenario, the random errors are added both in the simulated observations and T and Q background profiles. A mean profile of cloud water and rain is used as the cloud/rain background. In addition, a smaller observation error is adopted. The results are shown in Figure 7. The mean cloud/rain profiles are plotted in the blue curves. We can see that the retrieval of cloud water is much better than that in Figure 6. More sensitivity tests indicate that both the mean cloud/rain background profiles and the smaller observation error play some role on the improvement. It is also noticed that the retrieval of rain is little affected. Adding noise to the observations and the T, Q background has little effect due to large cloud/rain signal from the observations.

When combining the cloud water and the cloud ice as the control variables with relevant instruments, 1DVAR also succeeds to retrieve them. We did attempt to retrieve more cloud variables (e.g., add cloud ice as one of the control variables) by introducing more relevant instruments (e.g., HIRS and AMSU-A) in the simulated radiances. However, it was not successful to retrieve the cloud ice even though cloud water and rain can be still well retrieved. It keeps challenging to simultaneously retrieve more than 3 hydrometeors.

5. Conclusions

Cloudy radiance assimilation scheme implemented in WRF-3DVAR can extract to some extent the cloud/rain information with a better rain analysis than cloud water. The warm-rain physical constraint limits its application for cloudy radiance assimilation in the real world. Even for a simulated situation, it can cause some trouble by creating unrealistically large T and Q increments while generating cloud/rain increments. It will be more natural to introducing physical constraint in a 4DVAR system. Incremental implementation of WRF-3DVAR is probably another limitation for cloudy radiance assimilation.

The potential of using individual hydrometeors as the control variables is explored in a non-incremental 1DVAR retrieval framework. 1DVAR retrieval of cloud water and rain profiles is overall successful with the simulated SSMIS radiances. Carefully designed background and observation error covariances were needed to achieve a better result even with the simulated observations. No unexpected large T and Q increments were generated with large innovations under cloud/rain conditions. A large number of iterations was noticed for reaching a good convergence with current quasi-Newton algorithm. Simultaneous retrieval of multiple hydrometeors (e.g., more than 2) still keeps challenging.

References

Bauer, P., P. Lopez, A. Benedetti, D. Salmond, and E. Moreau, "Implementation of 1D+4D-VAR assimilation of microwave radiances in precipitation at ECMWF, Part I: 1D-VAR," *Q. J. R. Soc. Meteorol.*, 132, 2277-2306, 2006.

Liu, Z. and Barker, D. M., 2006: Radiance Assimilation in WRF-Var: Implementation and Initial Results, 7th WRF Users Workshop, June 19-22, 2006, Boulder, Colorado, USA

McNally, A. P., J. C. Derber, W.-S. Wu, and B. B. Katz, "The use of TOVS level-1B radiances in the NCEP SSI analysis system," *Q. J. R. Meteorol. Soc.*, vol. 128, no. 585, pp. 2511-2525, 2002.

Xiao, Q., Y.-H. KUO, J. SUN, W.-C. LEE, AND D. M. BARKER, "An Approach of Radar Reflectivity Data Assimilation and Its Assessment with the Inland QPF of Typhoon Rusa (2002) at Landfall", J. Appl. Meteor. and Clim., 46, 14–22, 2007.